Journal of the European Ceramic Society **10** (1992) 283–289

Densification and Microstructural Development of Two Si_3N_4 Alloys During Hot Isostatic Pressing

Daniel Sordelet*

GTE Laboratories Incorporated, 40 Sylvan Road, Waltham, Massachusetts 02254, USA

(Received 5 September 1991; accepted 29 November 1991)

Abstract

The densification and microstructural development of two Si_3N_4 alloys (AY6 and PY6) was observed by performing draw trials at various stages during a hot isostatic pressing (HIPing) cycle. The compositional differences produced differing densification rates; however, the α- to β-Si_3N_4 transformation rates were quite similar for the two materials. The fracture toughness of the AY6 was found to increase with increased β-Si_3N_4 content.

Die Verdichtung und die Gefügeentwicklung zweier Si_3N_4-Legierungen (AY6 und PY6) wurden für verschiedene Stadien des HIP-Zyklus (Heiß Isostatisches Pressen) verfolgt, indem jeweils Stichproben untersucht wurden. Der Unterschied in der Zusammensetzung beider Materialien führt zu unterschiedlichen Verdichtungsraten. Die Umwandlungsgeschwindigkeit von α-zu β-Si_3N_4 ist in beiden Materialien jedoch sehr ähnlich. Es wurde festgestellt, daß die Bruchzähigkeit von AY6 mit steigenden Anteil an β-Si_3N_4 zunimmt.

La densification et la développement microstructural de deux alliages à base de Si_3N_4 (AY6 et PY6) ont été observés en faisant des prélèvements à différents stades du cycle de pressage isostatique à chaud (HIP). Les différences de composition produisent différents taux de densification; malgré cela les taux de transformation de α- en β-Si_3N_4 ont été assez similaires pour les deux matériaux. On a observé que la résistance à la fracture du AY6 augmente avec la proportion de β-Si_3N_4.

* Present address: Ames Laboratory, 107 Metals Development, Iowa State University, Ames, IA 50011, USA.

1 Introduction

Si_3N_4 alloys are being developed and studied primarily for use in heat engine applications. Injection molding is one of the key shapemaking techniques to form many of the complex-shaped components, e.g. turbocharged, axial and radial gas turbine rotors.[1,2] Densification of injection-molded Si_3N_4 ceramics is frequently accomplished by the ASEA hot isostatic pressing (HIPing) process.[3–5]

The two Si_3N_4 alloys discussed in this paper are GTE AY6 (Si_3N_4 + 6 wt% Y_2O_3 + 1·5 wt% Al_2O_3) and GTE PY6 (Si_3N_4 + 6 wt% Y_2O_3). Processing conditions for HIPed Si_3N_4 materials are established to ensure complete densification and proper Si_3N_4 crystallinity and grain boundary phases. Previous characterization studies[6] of HIPed materials have been typically carried out on fully processed material after the final microstructural phase assemblage is fixed. The current study deviates from the normal post-process characterization by examining the densification and microstructural development of AY6 and PY6 materials during a typical HIPing cycle.

2 Experimental Procedures

2.1 Materials

The silicon nitride powder used (the AY6 and PY6 formulations) for this study is a blend of SN-E03 and SN-E10 (Ube Industries, Ube City, Japan) grades. The oxygen impurity content of the blend is approximately 0·90%, as measured by the vendor. The sintering aids, Y_2O_3 and Al_2O_3, were obtained from Molycorp Incorporated (Louviers, CO) and Reynolds Metal Company (Richmond, VA), respectively.

Journal of the European Ceramic Society 0955-2219/92/$5.00 © 1992 Elsevier Science Publishers Ltd, England. Printed in Great Britain

The powder-milling, binder-incorporation (compounding), and injection-molding procedures were as described in Refs 7 and 8. The AY6 samples were injection molded as oversize 50 × 4 × 3 mm flexure bars, and the PY6 samples were 25 mm in diameter × 70 mm long pieces sectioned from the ends of injection-molded tensile bar blanks. Three AY6 and PY6 samples were HIPed at each draw trial condition.

2.2 Characterization techniques

The primary quantitative data of interest were density and β-Si_3N_4 crystalline content. Densities were measured by the water immersion method; proper care was taken to accurately measure the saturated weights of samples with residual porosity. Sections of HIPed samples were crushed to pass through a 320 mesh sieve and packed into shallow mounts for X-ray diffraction (model 4226-R, Phillips, Eindhoven, The Netherlands). The three most intense α- and β-Si_3N_4 peaks were scanned to determine the relative fraction of each crystalline phase. One AY6 and PY6 powdered specimen from each draw trial condition was examined.

SEM (Model JX840, JOEL Ltd, Tokyo, Japan) analysis of polished and etched samples was used to follow the microstructural development of the AY6 and PY6 samples.

Indentation fracture toughness (IFT) measurements were performed on dense (>98% theoretical) AY6 samples after polishing, but prior to etching. Five Vickers indents at 10 kg loads were made on each sample analyzed; the results discussed later are expressed as the average of the five measurements.

2.3 Draw trial procedure

In their discussion of the ASEA glass encapsulated HIPing process, Adlerborn *et al.*[9,10] teach that the green ceramic body must be embedded in a low viscosity melt before the application of high-pressure gas. Typical glasses used in HIPing achieve the desired pressure transmitting viscosity, e.g. 10^4 to 10^6 poise, in the range of 1000 to 1300°C. Once a suitable temperature within this range is achieved and maintained for a sufficient time to ensure complete encapsulation of the ceramic body, the high-pressure gas is applied to the system. The level of pressure introduced at this initial stage can obviously vary greatly. It can be an intermediate value that will increase within the closed system as temperature increases or it can be a fixed level that will be maintained and controlled as the temperature increases. The magnitude and method of the pressure application will be specific to the materials being processed.

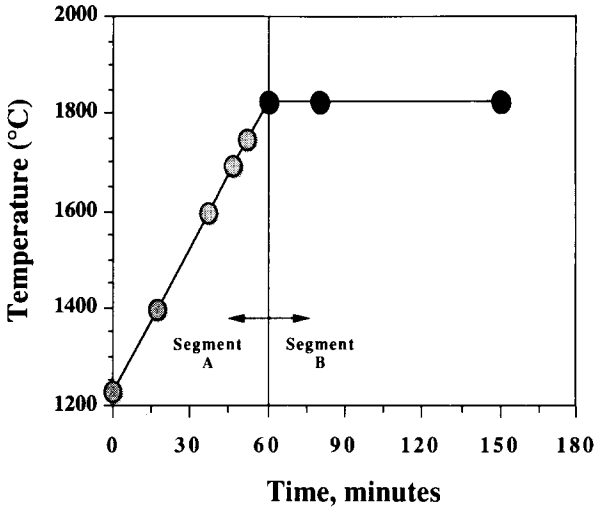

Fig. 1. Schematic illustration of times when HIPing draw trials were performed. Circles denote intermediate times when cycle was stopped.

In the current study, a series of seven draw trials were performed during two consecutive HIPing controller segments. The first segment, Segment A, is characterized by a 60 min ramp from 1230°C to the final densification temperature, 1825°C. 1230°C is in the range discussed above for the initial high-pressure application. The pressure applied at 1230°C is 138 MPa, and increases 50% during the 60 min ramp from 1230°C to 1825°C. The subsequent controller segment, Segment B, is an isothermal soak at 1825°C; the ultimate pressure achieved at 1825°C is maintained during the soak period.

The seven individual draw trials were performed by interrupting Segment A four times during the 60 min ramp from 1230°C to 1825°C, and by stopping Segment B after three hold times at 1825°C. The times at which each HIPing run was stopped are illustrated schematically in Fig. 1. Once the desired intermediate ramp temperature (Segment A) or soak time (Segment B) was reached, the temperature was rapidly decreased to <1000°C; typical ramp cooling times were between 10 and 30 min.

3 Results and Discussion

3.1 Densification behavior

The presence of 1·5 wt% Al_2O_3 in AY6 results in an increased densification rate compared to the PY6 material. Figure 2 shows the densities achieved by both compositions under the experimental conditions studied. The AY6 samples were >98% dense by 1700°C in Segment A, while the PY6 parts did not

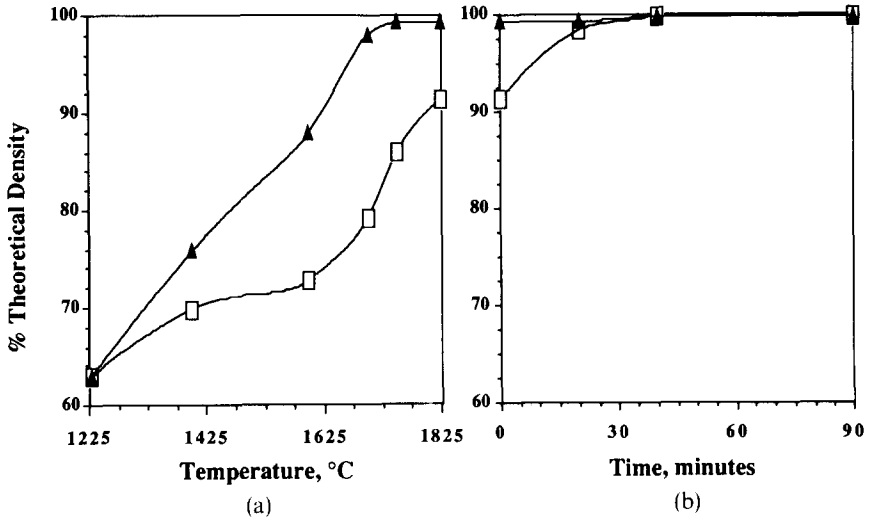

Fig. 2. Densities achieved by AY6 (▲) and PY6 (□) samples at each intermediate time during (a) Segment A and (b) Segment B.

reach an equivalent density until approximately 20 min at 1825°C in Segment B. Although full density is achieved for both materials after 90 min at 1825°C in Segment B, it is important to recognize that each composition actually sees very different heat treatments after complete consolidation. Fully dense AY6 material is exposed to a 13 min ramp from 1700°C to 1825°C in Segment A, and then a full 90 min soak at 1825°C in Segment B. In contrast, dense PY6 material is maintained at 1825°C for only 60–70 min in Segment B. Intuitively, differences in material properties between AY6 and PY6 should

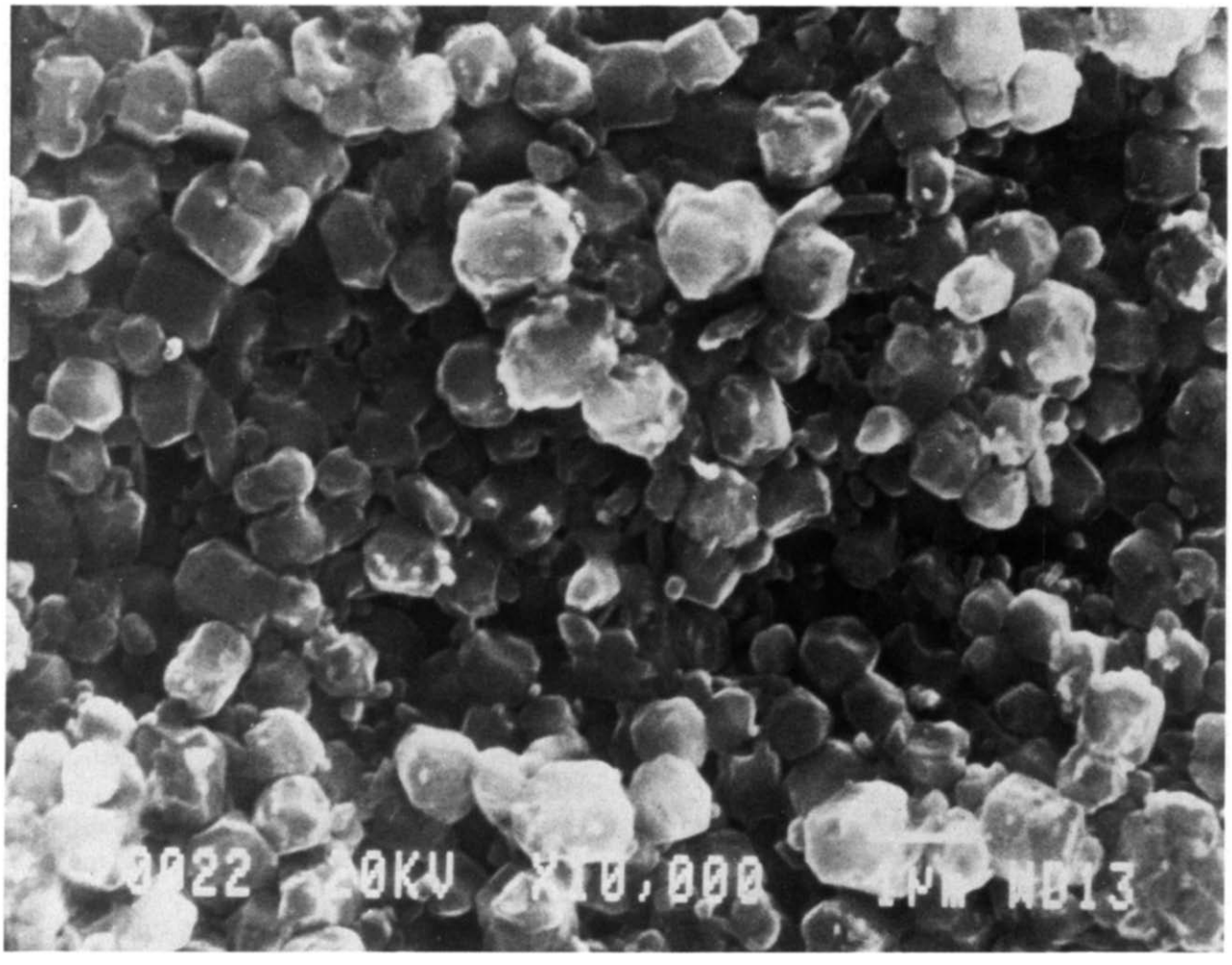

Fig. 3. Polished and etched SEM micrograph of 98% dense AY6 sample HIPed to 1700°C in Segment A.

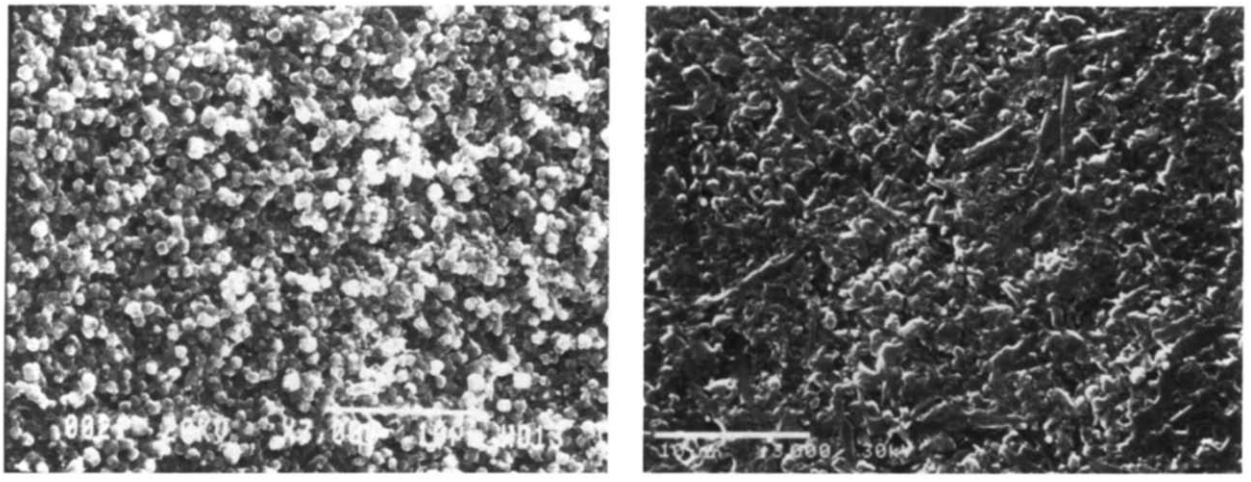

(a) (b)

Fig. 4. Polished and etched SEM micrographs of 98% dense AY6 and PY6 samples HIPed to the following intermediate times: (a) AY6 to 1700°C in Segment A and (b) PY6 for 20 min at 1825°C in Segment B.

be related in part to their contrasting post-consolidation thermal treatments.

The grain structure of the 98% dense AY6 sample interrupted at 1700°C is shown in Fig. 3. The original equiaxed particle morphology of the SN-E03 and SN-E10 Si_3N_4 particles is still visible. In this particular sample area, several very small acicular crystals have developed. These are most likely to be β-Si_3N_4. As discussed later, the measured β-Si_3N_4 content at 1700°C is about 7%. The mechanism of consolidation of this material around these temperatures is then presumably particle rearangement via liquid phase formation between Si_3N_4 grains.[11] The phenomenon of the α-Si_3N_4 dissolution into the liquid grain boundary phase and reprecipitation as β-Si_3N_4 does not appear to be a significant contribution to final densification, even though it may be occurring simultaneously with particle rearrangement, to a very small degree.

As shown in Fig. 2, the PY6 samples densified more slowly than the AY6 material. The PY6 samples were only 91% dense at the conclusion of Segment A. SEM mounts were not prepared from these porous specimens. X-Ray diffraction results suggest that only a small fraction of β-Si_3N_4 grains are present in these low density samples. A noteworthy difference between the AY6 and PY6 samples is the grain structure developed once samples approach 98% density. Figure 4 compares the AY6 microstructure developed at 1700°C in Segment A to that of the PY6 material formed at 1825°C for 20 min. The AY6 material is still fine grained, with few visible acicular β-Si_3N_4 crystals, while the PY6 sample has clearly experienced β-Si_3N_4 development and substantial grain growth. As discussed in the next section, the β-Si_3N_4 fractions of the 1700°C AY6 and 1825°C/20 min PY6 materials are about 7% and 67%, respectively.

3.2 Microstructural development

Contrasting densification behavior between AY6 and PY6 was expected and observed. However, the α- to β-Si_3N_4 transformation characteristics of the two materials, with respect to time and temperature, are quite similar. Figure 5 illustrates the quantitative development of β-Si_3N_4 crystals, as determined by XRD, in both materials throughout Segment A and B. Under the given experimental HIPing conditions, the transformation kinetics appear to be equivalent. Also, below 1825°C, the transformation appears quite sluggish. Since a rate-controlled process like this will be governed by both time and temperature constraints, it appears that temperatures of the order of 1825°C are required to drive this transformation in these particular materials within a reasonable period of time. Although not fully substantiated by the available data, it appears that below this temperature, no significant β-Si_3N_4 forms, but densification can still readily proceed, primarily via particle rearrangement. Above this temperature, solution and precipitation occurs more rapidly, independent of the material's density.

Figure 6 displays the microstructural development of the AY6 samples at densities >98% of theoretical. Figures 6(a)–(c) appear porous, but this effect is grain pullout during polishing of the very fine-grained equiaxed structure; final polishing was done with 1 μm Al_2O_3. Nevertheless, the particle edge rounding, grain rearrangement, crystalline transformation and growth are apparent in the series. Figure 7 presents β-Si_3N_4 grains at their infancy. Figure 7(a), AY6 HIPed to 1750°C in

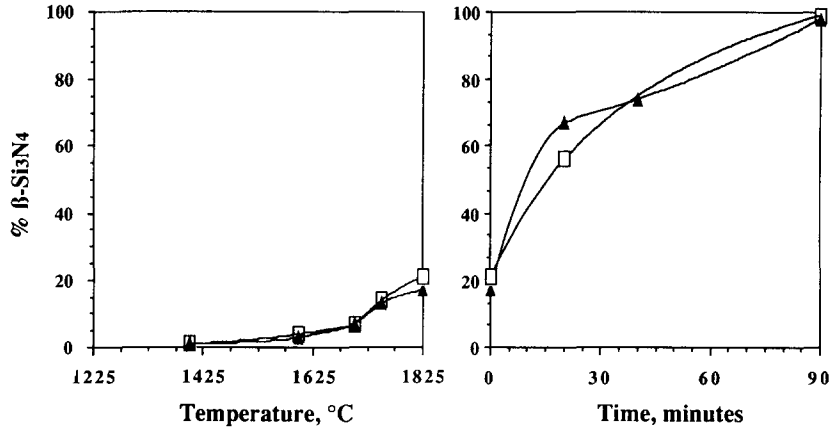

Fig. 5. Percentage of β-Si_3N_4 developed in AY6 (▲) and PY6 (□) samples at each intermediate time during (a) Segment A and (b) Segment B.

Segment A, was measured to have about 13% β-Si_3N_4. The subsequent AY6 draw trial sample, which was heated to 1825°C to end Segment A, is shown in Fig. 7(b), and reflects the increased β-Si_3N_4 nucleation at the higher temperature.

A comparative series of micrographs from the PY6 samples was not obtained as only the Segment B samples held for 20 and 90 min at 1825°C were >98% dense. Future work should also include intermediate conditions between these times. This

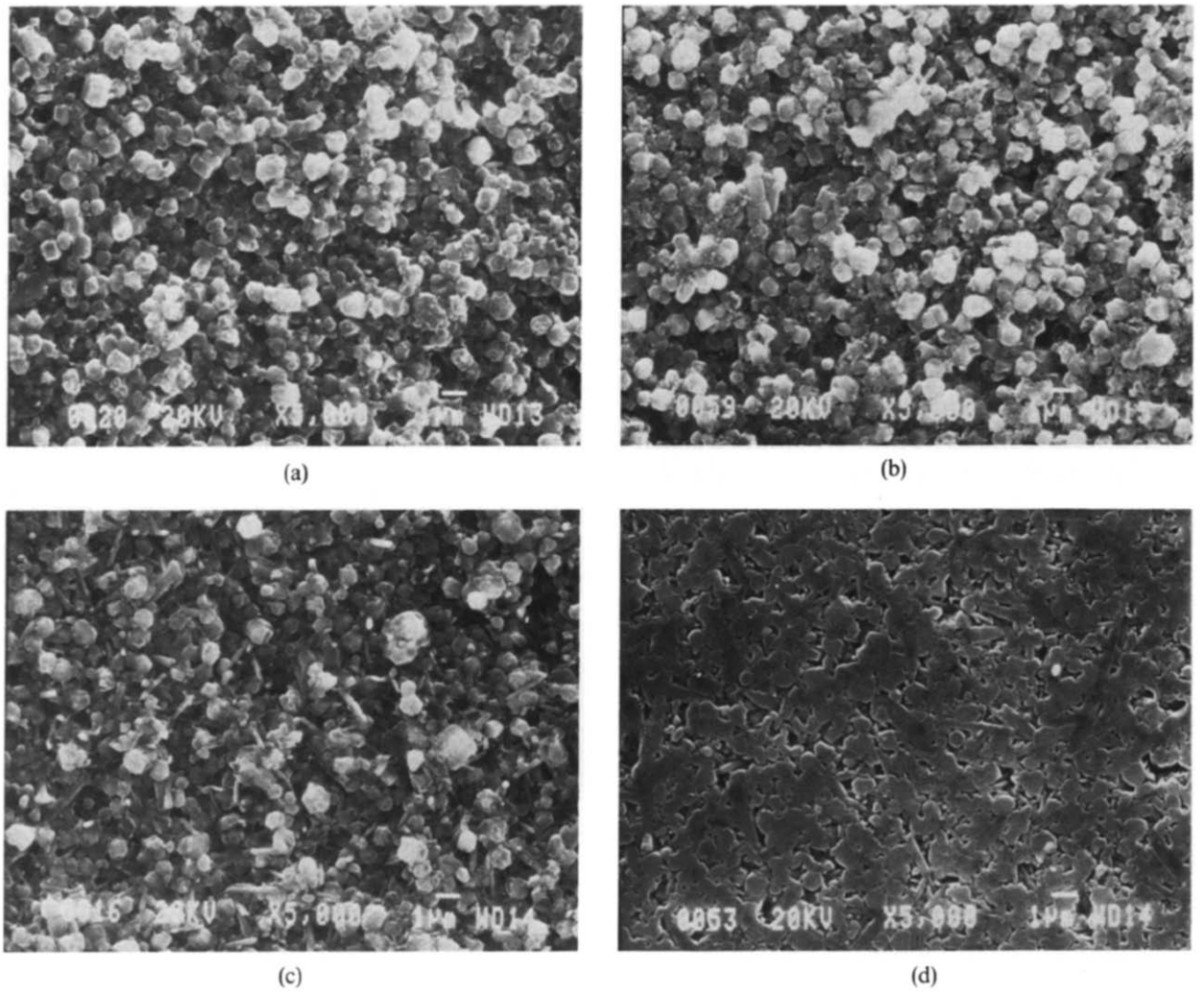

Fig. 6. Polished and etched SEM micrographs of AY6 samples HIPed to (a) 1700°C, (b) 1750°C, (c) 1825°C and (d) for 20 min at 1825°C.

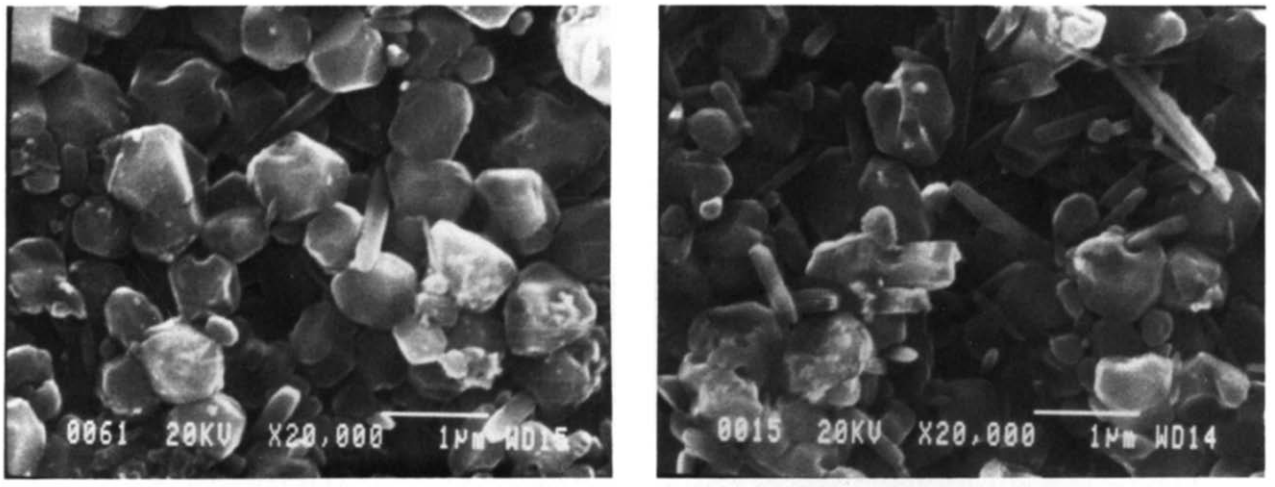

Fig. 7. Polished and etched SEM micrographs of AY6 samples HIPed to (a) 1750°C and (b) 1825°C, illustrating early β-Si_3N_4 nucleation and growth.

would be particularly interesting as these conditions are above a temperature that favors the α- to β-Si_3N_4 transformation in the PY6 material studied.

3.3 Indentation fracture toughness (IFT)

Samples HIPed under the conditions that produced >98% dense AY6 and PY6 materials were polished and indented to measure fracture toughness. Crack deflection in silicon nitride, and hence fracture toughness, is known to be a strong function of grain size and shape.[6,12] In Si_3N_4 ceramics, grain size can be related directly to the β-Si_3N_4 population. Therefore, a relationship between fracture toughness and β-Si_3N_4 content, with all else being equal, should exist. Figure 8 suggests that AY6 fracture toughness is indeed a function of the material's β-Si_3N_4 content. The figure should not be interpreted as showing that the value of 4·8 MPa × $m^{1/2}$ at 100% β-Si_3N_4 is an upper limit. Further increases in toughness may be achievable after full conversion by continued controlled grain growth of the β-Si_3N_4 crystals. The PY6 results, although based on only two conditions sufficiently dense for testing, are also shown in Fig. 8. The general trend toward higher toughness with increasing β-Si_3N_4 content is again observed.

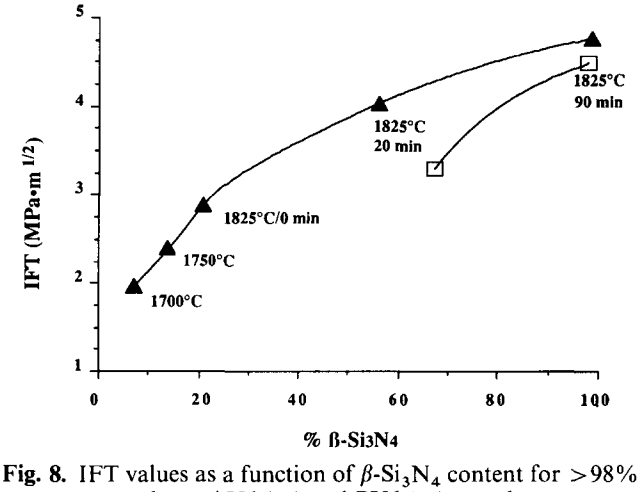

Fig. 8. IFT values as a function of β-Si_3N_4 content for >98% dense AY6 (▲) and PY6 (□) samples.

4 Conclusions

The characterization of AY6 and PY6 injection-molded material densified at intermediate temperatures during a standard HIPing cycle revealed several interesting features. As expected, AY6 densifies faster than PY6. The transformation kinetics of the α- to β-Si_3N_4 conversion, however, appeared to be similar for both compositions. The transformation progressed more rapidly around 1825°C and the limited data suggest that it is independent of the material's density. SEM micrographs illustrated the microstructural development from discrete particle rearrangement through β-Si_3N_4 nucleation and growth. Fracture toughness of the AY6 material correlates well with its β-Si_3N_4 content.

Acknowledgements

This work was supported, in part, by the US Department of Energy, Assistant Secretary for Conservation and Renewable Energy, Office of Transportation Systems, as part of the Advanced Turbine Technology Applications Program through a subcontract from Allison Gas Turbine Division of General Motors, Purchase Order No. H926604. The

assistance of Arlene Hecker in IFT sample preparation and measurement is gratefully appreciated. Mike Downey and Lou Steriti are acknowledged for their quantitative XRD efforts. George Werber is responsible for the SEM micrographs.

References

1. Bandyopadhyay, G., French, K. W., Sordelet, D. J. & Mahoney, F. M., Fabrication and evaluation of silicon nitride heat engine components. In *Proceedings of the 3rd International Symposium on Ceramic Materials and Components for Engineers*. Las Vegas, NV, USA, 27–30 November, 1988, pp. 1397–406.
2. Bandyopadhyay, G. & French, K. W., Fabrication of near-net-shape silicon nitride parts for engine application. ASME Paper 86-GT-11, 1986.
3. Neil, J. T., Bandyopadhyay, G., Sordelet, D. J. & Mahoney, F. M., Development in injection-molded silicon nitride turbine components. ASME Paper 90-GT-186, 1990.
4. Busovne, B. J. & Pollinger, J. P., Development of silicon nitride engine components for advanced gas turbine applications. ASME Paper 89-GT-259, 1989.
5. McEntire, B. J., Taglialavore, A. P., Heichel, D. N., Johnson, J. W., Bright, E. & Yeckley, R. L., ATTAP ceramic component development using Taguchi methods. In *Proceedings of the Twenty-sixth Automotive Technology Contractors' Coordination Meeting*. Society of Automotive Engineers Inc., Warrendale, PA, 1989, pp. 289–300.
6. Sordelet, D. J., Neil, J. T., Mahoney, F. M. & Hecker, A. H., Development of injection-molded gas turbine components: Investigation into toughening GTE PY6 Si_3N_4. ASME Paper 91-GT-65, 1991.
7. Neil, J. T., French, K. W., Quackenbush, C. L. & Smith, J. T., Fabrication of turbine components and properties of sintered silicon nitride. ASME Paper 82-GT-252, 1982.
8. Bandyopadhyay, G. & French, K. W., Fabrication of near net shape components for engine applications. *J. Engineering for Gas Turbines and Power*. **108** (1986) 536–9.
9. Adlerborn, J. Larker, H., Mattsson, B. & Nilsson, J., Method of manufacturing an object of metallic or ceramic material. US Patent No. 4,446,100, 1 May 1984.
10. Adlerborn, J., Larger, H., Mattsson, B. & Nilsson, J., Method of manufacturing an object of metallic or ceramic material. US Patent No. 4,478,789, 23 October 1984.
11. Lange, F. F., Fabrication and properties of dense polyphase silicon nitride. *J. Am. Ceram. Soc.*, **62**(12) (1983) 1369–74.
12. Buljan, S. T., Baldoni, G. & Huckabee, M., Si_3N_4–SiC composites. *Am. Ceram. Soc. Bull.*, **66**(2) (1987) 347–52.